energies

Article

The Concept of Spatial Reliability Across Renewable Energy Systems—An Application to Decentralized Solar PV Energy

Athanasios Zisos , Dimitrios Chatzopoulos and Andreas Efstratiadis *

Laboratory of Hydrology and Water Resources Development, School of Civil Engineering, National Technical University of Athens, Heroon Polytechneiou 9, 15780 Zographou, Greece; cv19090@mail.ntua.gr (D.C.)
* Correspondence: andreas@itia.ntua.gr

Abstract: Decentralized planning of renewable energy systems aims to address the substantial spatiotemporal variability, and thus uncertainty, associated with their underlying hydrometeorological processes. For instance, solar photovoltaic (PV) energy is driven by two processes, namely solar radiation, which is the main input, and ambient temperature, with the latter affecting the panel efficiency under specific weather conditions. The objective of this work is to provide a comprehensive investigation of the role of spatial scale by assessing the theoretical advantages of the distributed production of renewable energy sources over those of centralized, in probabilistic means. Acknowledging previous efforts for the optimal spatial distribution of different power units across predetermined locations, often employing the Modern Portfolio Theory framework, this work introduces the generic concept of spatial reliability and highlights its practical use as a strategic planning tool for assessing the benefits of distributed generation at a large scale. The methodology is verified by considering the case of Greece, where PV solar energy is one of the predominant renewables. Following a Monte Carlo approach, thus randomly distributing PVs across well-distributed locations, scaling laws are derived in terms of the spatial probability of capacity factors.

Keywords: renewable energy; distributed systems; spatial reliability; scale; capacity factor; solar PVs

check for updates

Citation: Zisos, A.; Chatzopoulos, D.; Efstratiadis, A. The Concept of Spatial Reliability Across Renewable Energy Systems—An Application to Decentralized Solar PV Energy. *Energies* **2024**, *17*, 5900. https://doi.org/10.3390/en17235900

Academic Editor: Olabi Abdul-Ghani

Received: 22 October 2024
Revised: 13 November 2024
Accepted: 22 November 2024
Published: 25 November 2024

1. Introduction

The large-scale adoption of variable renewable energy sources (VRES) and the need for their more efficient utilization are propelled by the urgency of satisfying the ever-growing electricity demand, advancing sustainable development, addressing climate concerns, and reducing greenhouse gas (GHG) emissions associated with fossil fuels [1]. Among these renewable sources, solar energy is arguably the most abundant, easily available, and versatile, allowing for both direct and indirect conversion into various forms of energy. As such, various solar energy projects have been globally established, with great emphasis on solar photovoltaic (PV) ones, which currently exceed 1.4 TW of total installed power capacity [2], while their market share is expected to increase to up to 70% by 2030 [3]. Remarkably, the rather increased adoption rate of solar PVs is not only attributed to the sharp decrease in their overall cost, but also to the fact that the total annual solar radiation received by Earth is more than 7500 times the world's primary energy consumption [4], meaning that there is still a significant amount of "untapped" solar potential.

However, the broader expansion of solar energy applications is mainly hindered by the high levels of uncertainty that power production inherits from the resource itself due to multiple factors, with the primary one being its stochastic and intermittent nature. Accurate estimation of both the incident solar radiation and the output power of a specific region remains a formidable challenge. Therefore, the planning, design, and implementation of solar energy projects should account for both the spatial and temporal variability of solar radiation [5]. Part of this variability is deterministic since it is attributed to seasonal and intra-day phenomena [6] caused by the Earth's rotation and its orbital motion around the sun. These are fully explained by the location (i.e., latitude and longitude) and predictable astronomic variables that are expressed as periodic functions (e.g., solar altitude and declination). At the same time, solar power is also influenced by topography [7,8], which is expressed in terms of underlying geographical properties at regional and local scales (i.e., slope, aspect, altitude, and shading). On the other hand, atmospheric conditions, such as clouds, aerosol particles, water vapors, and ozone [9], which absorb, reflect, and scatter solar radiation [10], are random processes that strongly modify the known pattern of global radiation fields. Furthermore, the output power is subject to additional random processes that are attributed to microclimatic conditions, e.g., ambient temperature, humidity, and dust, which may significantly affect the PV panels' efficiency, thereby reducing the output power [11–14].

To address the spatiotemporal variabilities of solar radiation, distributed (also termed as decentralized) PV systems have been introduced, shifting the traditional energy paradigms rooted in centralized and continuous energy production by integrating numerous spatially dispersed, self-sufficient small-scale configurations (either as standalone or grid-connected) [15]. Such systems have been gaining popularity, with their installed capacity now accounting for almost half of the total solar PV growth [16]. This increase in distributed PV adoption can be attributed to their ability to leverage geographical smoothing, which reduces output power variability and uncertainty. More specifically, solar power's inherent smoothing is a phenomenon associated with the spatial scale that lies beneath the varying climatic and cloud conditions (e.g., cloud coverage is typically not homogeneous), and aerosols (haze/pollution) across geographically dispersed regions [17,18]. The geographical aggregation of distributed PV systems on a large scale generates a smoother and less intermittent power output with significantly reduced fluctuations (both positive and negative) compared with that of an individual PV plant [19]. This indicates that at any given time, the reduced power output derived from regions where incident radiation may exhibit relatively lower values is expected to be offset by better-performing regions that simultaneously receive higher radiation values.

From a technical viewpoint, locally based distributed energy systems offer enhanced efficiency and more flexible (demand-side) management compared to centralized ones, also reducing reliance on the latter [20,21]. In particular, distributed systems have the ability to deliver the same electricity services provided by centralized ones while also being capable of providing additional locational value, namely, by (a) delivering energy in regions that experience high marginal losses, (b) providing reliable power injections that reduce net load consumption in regions that would otherwise require network upgrades, and (c) supplying energy during network failures [22]. Importantly, a combined power supply system consisting of both centralized and distributed configurations can significantly increase the overall performance of key electricity service delivery.

The optimal design of distributed PV systems is a multiparametric exercise, accounting for siting issues (i.e., orientation and tilt angle), ensuring that candidate locations are less susceptible to power curtailment factors (i.e., high temperatures [12] and dust accumulation [23,24]), sizing criteria (to match load demand), selection of appropriate module types and technologies, and associated installation and operational costs. Thus far, traditional design approaches have focused on the spatial distribution of solar radiation [25–27] and its respective impact on power production [28]. These analyses typically aim to identify the "best" locations for PV installations, following multi-criteria decision-making (MCDM) techniques that account for various factors (e.g., slope, land suitability, distance to water resources, policy support, etc.) [29,30]. Nevertheless, while the optimal allocation of PV systems is crucial for maximizing energy efficiency and cost-effectiveness, an equally important goal is to ensure reliability, as it is pertinent to their long-term performance and sustainability.

In the classical systems analysis context, reliability is a key probabilistic metric, defined as the frequency of the successful delivery of requested system services. In the case of PV systems, this translates to the adequacy and time availability of power delivery to match the load demand. Consequently, common reliability indices in the energy literature emphasize its temporal dimension, as further outlined herein.

On the other hand, studies that delve into the concept of spatial reliability are very limited; to the authors' knowledge, this term has only been used so far in the assessment of power transmission network lines [31] and 5G communication networks [32,33].

The objective of this work is to expand the major notion of the temporal reliability of energy systems to the space domain. In this vein, it introduces the concept of *spatial reliability* as a means of quantifying, in probabilistic terms, the benefits of decentralized configurations, with a specific focus on PV systems. This may serve as a background feasibility analysis for the strategic development of PV energy on a large scale (e.g., national or regional). Its practical implementation in a Monte Carlo context is verified by taking as an example the case of PV development in Greece, a country where solar energy is one of the predominant renewables and PV installations prosper. This analysis allows for assessing the spatial uncertainty in PV power production and extracting the associated scaling laws in terms of capacity factor values with respect to spatial dispersion.

This article is organized as follows. Section 2 presents a brief overview of works concerning the optimal spatial distribution of VRES systems, with particular emphasis on Modern Portfolio Theory (MPT), a well-established methodology that accounts for multiple factors to provide an optimal frontier of alternative configurations. Section 3 delves into reliability within VRES systems, highlighting the associated assessment methodologies and typical indices considered. Section 4 comprehensively introduces the concept of spatial reliability in VRES systems and suggests suitable probabilistic methods for its quantification. Section 5 presents the study area and the methodology used to verify the proposed concept. Finally, Section 6 discusses considerations for future research, and Section 7 summarizes the key outputs of this research.

2. The Rationale of Optimal Solar PV Spatial Distribution

Overall, the site selection and design of energy systems are multidimensional and intricate procedures that involve multiple conflicting assessment criteria and alternatives [34]. From an investor perspective, the optimal location of the energy system maximizes electricity generation at minimum costs (investment and operation) [35]. However, this spatial allocation opts for the "best" performing sites that exhibit the highest resource exploitation potential, disregarding factors that may be technical (e.g., grid constraints), as well as political-geopolitical (e.g., energy security, energy autonomy, and international agreements). In fact, it has been indicated that solely investing in the most productive areas is not the best policy, as these solutions often yield significant variability in power output. On the contrary, the spatial dispersion of assets reduces variability [36–38], especially when combining less productive locations with the best performing ones, which can improve the overall risk-production pairing [39].

The benefits of energy systems' spatial dispersion and the associated geographical smoothing effects can be captured by the Modern Portfolio Theory (MPT). The MPT, initially introduced by Markowitz [40], is a widely accepted methodology employed in energy planning and is typically framed as an investment selection problem that accounts for the siting and sizing of renewable energy systems. In contrast to previously used methodologies (e.g., individual least cost alternative), MPT is based on solving an optimization problem subject to different constraints, whose objective function seeks to either minimize the cost or risk of the associated portfolio or maximize the assets' return or yield. Most MPT studies consider the portfolio capacity factor (CF) to be the "yield", the standard deviation of power output to be the "risk" and the installed capacity to be the "budget" [41–43]. The optimization determines the efficient cost-risk frontier, considering that power production assets can be defined in terms of cost or return and economic risk for each alternative technology [38]. This Pareto-shaped frontier indicates that portfolios located on the right edge are not optimal, whereas portfolios on the left edge are infeasible.

Many MPT applications for VRES can be found in the literature. The first application of MPT in energy planning was conducted by Bar-Lev and Katz, who analyzed the relationship between the U.S. electric utility industry and fossil fuel procurement [38,44]. Several MPT studies have focused on examining blended portfolios of wind and solar, utilizing the complementarity of the two sources [45,46], also considering that they are present in both minimum-risk and cost-efficient portfolios [47]. For instance, Shahriari and Blumsack [41] identified portfolios (solar, wind, and blended ones) at various spatial and temporal scales to quantify capacity benefits in various parts of the electrical grid in the Eastern United States. Hu et al. [43] employed MPT to capture geographical smoothing effects for China's future power system, assessing the return and volatility of each VRE asset in China. Castro et al. [48] propose several improvements in the traditional MPT approach, such as considering generation cost instead of installed capacity as one of the objectives, and employ this model in Brazil. Interestingly, their methodology's new efficient frontier has a much shorter range of standard deviation values, thus proving that many portfolios obtained from traditional MPT approaches exhibit higher probabilities of under-production. Furthermore, Mauleón [39] studied the optimal spatial combination of PVs in Spain and determined that participation of wind energy in solar portfolios for as low as 10% can significantly reduce the variability of total generation.

Unlike the aforementioned studies that consider blended portfolios of wind and solar, to the authors' knowledge, there are limited works on the optimal allocation of distributed PV systems over large regions (e.g., at the national or regional scale). Among these, Urquhart et al. [49] performed a multi-objective analysis of the optimal allotment of PVs across four sites in Lanai, Hawaii. More recently, Carpio [35] formed an optimal PV portfolio for distributed power generation that featured the highest productivity and least intermittency across Brazil. Lastly, Pillot et al. [50] formulated an integrated GIS optimization framework that accounts for the spatiotemporal dimension of PV planning.

3. Reliability Standards Within Energy Systems

3.1. Generic Definitions

In general, reliability is a characteristic of a system driven by uncertainties, and is expressed as the probability that it will perform its required function under specific conditions for a stated time interval [51]. Following the rationale of Koutsoyiannis [52], this typically refers to either a system's structural integrity or its service delivery adequacy. In the second case, the concept of reliability, a, is mathematically expressed as follows:

$$a := 1 - \mathcal{P}[Y(t) < D(t); t \in \mathcal{T}] =: 1 - \beta \tag{1}$$

where $Y(t)$ and $D(t)$ represent the "yield" and "demand", respectively, at time t, within a specific time period $\mathcal{T}$, and β is its complementary notion, referred to as probability of failure or risk. Often, the problem is posed inversely, thus requiring the determination of a constant demand to be fulfilled at a given reliability level. This quantity, which is expressed as a single value or by means of a repetitive pattern (e.g., seasonal), is also referred to as "safe", "firm" or "reliable" yield.

Both the forward and inverse problems do not have analytical solutions, except for the specific formulations of Equation (1), in which the yield $Y(t)$ has a simple probabilistic structure (e.g., it is normally distributed), and the demand is constant, i.e., $D(t) = d$. Otherwise, the most effective option is the use of Monte Carlo approaches, thus representing the randomly varying processes $Y(t)$ and $D(t)$ through a simulation model, and accounting for the probabilistic/stochastic regime of failure events (i.e., deficits) and their associated frequencies of occurrence [53]. In this context, and in order to reduce model complexity and computational burden, the continuous time domain is handled in discrete terms, thus dividing $\mathcal{T}$ into n equal time intervals, Δt, and estimating reliability empirically, by counting the number of deficits:

$$a := 1 - n_d / n \tag{2}$$

where n_d is the number of failed time steps, in which the yield is less than the demand.

3.2. Energy Reliability

With the constantly increasing penetration of VRES into the global electricity mix, and considering their associated uncertainties, it is imperative to transform traditional electrical power systems to ensure reliable power delivery. According to the U.S. Office of Energy Efficiency and Renewable Energy [54], energy reliability is defined as a power system's ability to withstand instability, uncontrolled events, cascading failures, or unanticipated loss of system components, thus ensuring seamless power delivery, even under physical and cyber events that cause power disruptions. Similarly, in order to frame the reliability problem in power systems, researchers at the National Renewable Energy Laboratory (NREL) argue that all three R's, namely resource adequacy, operational reliability, and resilience, must be present [55].

In this context, the reliability of energy generation from VRES has been thoroughly investigated in the literature, with the first study taking place in 1978 by Kahn, who discussed the reliability benefit of geographically dispersed wind generation due to the spatial correlation of sites [56,57]. This cumulative effort has helped shape the current reliability standards in power delivery in industrialized countries, which are very high, typically targeting no more than 2–3 h of unplanned outages per annuum (translating to ~99.97% reliability) [58] or no more than one day of unmet electricity demand and, in some cases, only one loss of load event in 10 years—the so-called "1-in-10" standard (i.e., 99.97% and 99.9% reliability, respectively) [59,60].

The reliability of power systems is typically assessed in terms of adequacy by considering static conditions. This entails evaluating whether the system can meet the load demand and operational requirements, also considering the risks of failure [61] through a series of indices that measure the probability, severity, frequency, and duration of the expected load shedding [62].

Energy reliability assessment methodologies vary in the literature, both in terms of the employed models and indices considered. For instance, a common metric used in the literature since the early works of Kahn is the loss of load probability (LOLP), which is the probability of a system being unable to match the demand load at a given time. Another reliability metric pertinent to VRES generator integration into the electricity grid is the effective load-carrying capability (ELCC), which is defined as the additional constant load that can be met at the same reliability level as the original system [63]. A series of reliability indicators for hybrid renewable energy systems can also be found in the work of Jijian et al. [64], which are typically estimated through probabilistic model simulations.

Similarly, a concise overview of energy reliability studies, specifically related to PV systems, which is the renewable technology emphasized in this work, is provided herein. Kumar et al. [65] presented a survey on the reliability evaluation of electrical power systems when integrating VRES to conventional power systems, including solar PVs. De Oliveira and Borges [61] investigated the influence of PV generation on the reliability evaluation of distribution systems, considering irradiance and ambient temperature in the PV power output, as well as spatial smoothing effects. Abunima and Teh [66] proposed a novel reliability model that considers various inputs (e.g., weather conditions and detailed system architecture) to determine the time-varying failure rates of PV systems and their individual components. Zisos et al. [67] developed a stochastic simulation-optimization framework for the design of hybrid renewable energy systems (also including PVs), embedding reliability as a key performance metric. Lastly, of particular importance is the work of Singh et al. [55], who presented a comprehensive review of reliability assessment methodologies for grid-connected PV systems, outlining key reliability indices for analyzing their performance.

4. Introducing the Concept of Spatial Reliability

The previous section provided an understanding of how well the concept of reliability is established in the domain of energy systems, particularly after the large-scale expansion of renewables, albeit with a primary focus on the temporal scale. The benefits of spatial dispersion, such as leveraging the geographical smoothing phenomenon to reduce power output variability (already outlined in the Introduction), suggest that it is equally important to consider the *spatial dimension* of reliability. In fact, it is well recognized that the combination of spatial distribution and temporal complementarity of VRES systems can improve their overall reliability. On the one hand, temporal complementarity is observed between two or more energy sources, except when different technologies are utilized to harness the same energy source. Spatial complementarity, on the other hand, can also be observed with only one source. As such, the scarcity of one VRES in site x is complemented by its availability in site y, at the same time, t [68].

Specializing the generic mathematical context of Section 3.1, to the design and management of VRES systems, reliability may be expressed either as a forward problem (i.e., reliability of fulfilling a given energy demand) or an inverse one (i.e., a constant yield or yield pattern that can be achieved for a specific reliability level) [53]. This analysis, following the inverse problem, introduces the concept of spatial reliability in VRES systems, defining it as *the probability of achieving a guaranteed level of power production over a given region*. The generic mathematical expression of spatial reliability is similar to Equation (1) by substituting time index t with space index s, i.e.,:

$$a := 1 - \mathcal{P}[Y(s) < D(s); s \in \Omega] \tag{3}$$

where Ω denotes a certain spatial domain and $Y(s)$ and $D(s)$ refer to the energy yield and associated demand at a certain site, respectively. The energy yield can be expressed in terms of typical performance indices of power production systems. Similar to time-based reliability, while the space domain Ω is continuous, it is also handled as discrete, thus dividing Ω into sub-areas (e.g., by delineating a mesh grid) and accounting for an average performance metric of the energy source under study over each sub-area. An even simpler approach is to estimate this metric on a point basis, provided that the selected points ensure a satisfactory representation of the spatial variability of power production over the entire area of interest.

A typical metric for assessing the performance of renewable energy systems is the mean annual capacity factor, CF. This metric is generally defined as the ratio of the actual electricity production, E, to the theoretical maximum that can be produced by a project (or system of projects) of the total power capacity P_{max} during a given time interval, T:

$$CF = \frac{E}{P_{max}T} = \frac{\int_0^T P(t)dt}{P_{max}T} \tag{4}$$

In this context, the mean annual capacity factor contrasts the mean annual energy yield with its theoretical maximum value, assuming the continuous operation of the power system in its full capacity, for T = 8760 h.

The quantification of both the temporal and spatial reliability of VRES power production systems requires inputs that are inherently defined as stochastic since they are driven by randomly varying atmospheric processes (e.g., streamflow, wind speed, and solar radiation). As their conversion to power is subject to nonlinear dynamics, typically expressed in terms of empirical nomographs (e.g., efficiency curves) or even more complex procedures (the case of hydroelectric reservoirs), an analytical derivation of spatial reliability is impossible (the same stands with temporal reliability, as thoroughly discussed in [53]). In this vein, a Monte Carlo simulation (MCS) is considered an appropriate method for its quantification, as it is easily formalized through a numerical procedure that accurately represents real-world systems in probabilistic means.

The implementation of the spatial reliability concept in practice is demonstrated in the case of solar photovoltaic (PV) energy by considering Greece as the spatial domain of interest.

5. Proof of Concept: Distributed PV Energy in Greece

5.1. Study Area and Data

This section delves into verifying the theoretical expression of the spatial reliability of solar PV energy in a Monte Carlo context. The methodology is applied to the case of Greece, where solar energy is one of the predominant renewables. The PV power output is calculated through a simulation procedure that accounts for a typical commercial panel across 40 well-distributed locations driven by solar radiation and ambient temperature. This analysis considers an indicative commercial PV panel, the technical characteristics of which are summarized in Table 1.

Table 1. Technical characteristics of a typical PV module.

Nominal Power, P_{nom} (W)	**400**
Panel efficiency (%)	22.6
Operating temperature	−40 °C to +85 °C
Dimensions (mm)	1046 × 1690 × 40

The two input time series across the 40 locations (Figure 1) of interest are derived from satellite-based hourly weather data of 16 years length (2005–2020). These are retrieved from the Satellite Application Facility on Climate Monitoring (CMSAF) collaboration [69] through the Photovoltaic Geographical Information System (PVGIS) application [70]. The PVGIS portal provides solar radiation data at fine scales (spatial and temporal) using the Surface Solar Radiation Data Set Heliosat-2 (SARAH-2), with a spatial resolution of approximately 5 km (0.05° × 0.05°). This is of crucial importance, acknowledging the high demand for such data, combined with their scarce availability, mainly due to purchase and maintenance costs, as well as the calibration requirements of the associated equipment used for ground measurements [71]. Importantly, the calculation of solar radiation at ground level from satellite images for the CMSAF data is facilitated through comprehensive algorithms, also accounting for atmospheric data (i.e., water vapor, aerosols, and ozone), usually providing highly accurate results, with a few exceptions, as outlined by Lehneis et al. [72].

Figure 1. Map of Greece showing the 40 examined locations (source: Google Earth map, processed by the authors).

The acquired radiation and temperature PVGIS data were contrasted with ground observations from three meteorological stations operating close to the associated sites, exhibiting quite satisfactory similarities. Nevertheless, it is important to consider that discrepancies between the two data sources are expected and are attributable to the fact that satellite products offer gridded data, which refer to coarse spatial resolutions, compared to those of meteorological stations, which refer to point-specific measurements.

5.2. Methodology

The hourly solar power production is commonly treated as a linear function of incoming solar radiation, G. Once G exceeds the value of 1000 W/m^2, the PVs operate at their nominal power. In this context, the hourly PV power production is calculated using the following formula:

$$P_{hourly} = \begin{cases} n_{actual} \cdot G \cdot A_{panel}, & G < 1000\ W/m^2 \\ \frac{n_{actual}}{n_{nom}} P_{nom}, & G \geq 1000\ W/m^2 \end{cases} \quad (5)$$

where n_{nom} is the nominal (theoretical) efficiency of the PV panels, n_{actual} is the adjusted efficiency of the PV panels after considering temperature effects, G is the solar radiation (W/m^2), A_{panel} is the PV-occupied area (m^2), and P_{nom} is the nominal power, which is achieved under the so-called Standard Test Conditions (i.e., for a cell temperature of 25 °C, solar irradiance of 1000 W/m^2, and air mass of 1.5).

Temperature effects on solar PV production are well-studied in the literature, as they are one of the primary factors responsible for significantly degrading conversion efficiency by up to 12% [73–75]. More specifically, solar cell performance decreases as the temperature increases, fundamentally owing to the increased internal carrier recombination rates caused by increased carrier concentrations. Both the electrical efficiency and the power output of a photovoltaic (PV) module depend linearly on the operating temperature [11]. This analysis considers the traditional linear expression introduced by Evans and Florschuetz [76] to estimate the adjusted efficiency, n_{actual} as follows:

$$n_{actual} = \begin{cases} n_{nom}, & T_c \leq T_{ref} \\ n_{nom}\left[1 - a_{\mathcal{T}} \cdot \left(T_c - T_{ref}\right)\right], & T_c > T_{ref} \end{cases} \quad (6)$$

where n_{nom} is the nominal efficiency of the PV panels, and $a_{\mathcal{T}}$ is the power temperature coefficient (%/°C), denoting the rate of PV efficiency decrease for every unit increase in the ambient temperature above T_{ref} (which equals 25 °C in this case). This analysis considers $a_{\mathcal{T}}$ = 0.4, which is a typical value for conventional PV modules. Finally, T_c refers to the cell temperature and is calculated using the following formula:

$$T_c = T_{ambient} + \frac{NOCT - 20}{800} G \quad (7)$$

where $T_{ambient}$ is the ambient temperature (°C), G is the solar radiation (W/m^2), and $NOCT$ is the nominal operating cell temperature, which is defined as the temperature of the cell in a standard reference environment (i.e., ambient temperature of 20 °C, solar irradiance of 800 W/m^2, and wind speed of 1 m/s) [75]. In general, the $NOCT$ is constant for PV modules, and its value is provided by the manufacturer or determined from actual on-site measurements. However, for the purpose of this analysis, and in the absence of detailed information (which is beyond the objectives of this research), a constant value is applied for all sites; thus, $NOCT$ is set at 45 °C, which falls within the typical value range of 45 $\pm$ 2 °C for monocrystalline and polycrystalline PV modules [77].

The PV power potential of each location is expressed in dimensionless terms through the annual capacity factor as follows:

$$CF = \frac{E_{annual}}{P_{nom} \cdot 8760} \tag{8}$$

Particularly, in the case of VRES (including solar radiation), which are driven by randomly varying (i.e., stochastic) atmospheric processes, CF may be regarded as a macroscopic financial assessment metric since it contrasts the power system's response, and thus economic benefits, with its installed capacity, which is directly associated with the investment costs [78].

5.3. Baseline Scenario

To better understand the benefits of spatially dispersed PV systems, the individual power production for the selected locations is first estimated, which hypothetically corresponds to the state of centralized systems. This analysis is herein referred to as the "baseline" scenario. Table 2 summarizes the main outcomes in terms of the key statistical characteristics of the two input processes and the main output, i.e., the capacity factor, over the 40 examined locations. The detailed characteristics of each location are given in Appendix A.

Table 2. Key statistical characteristics (on an annual basis) of all quantities of interest across the 40 locations examined in Greece.

	Temperature (°C)	Solar Radiation (W/m^2)	Capacity Factor
Average	16.07	195.23	0.191
Standard deviation	2.21	12.45	0.013
Minimum	10.62	170.28	0.169
Maximum	18.92	219.50	0.214

The spatial variability of the centralized production is probabilistically expressed and visualized through the empirical probability curve (inverse cumulative distribution function-CDF) of the annual capacity factors across the selected locations. The curve data are derived by sorting the simulated capacity factor values in descending order and assigning an empirical exceedance probability to each value. In this respect, the vertical axis represents the PV power potential in terms of the capacity factor, and the horizontal axis represents the percentage of locations that can guarantee the corresponding capacity factors. If n is the size of the data (in our case, the number of locations), the empirical probability of exceeding the sorted value at position i is estimated through the Weibull plotting position, i.e.:

$$\mathcal{P}_i = \frac{i}{n+1} \tag{9}$$

To provide a continuous spatial probability model, the Kumaraswamy distribution function is utilized. This is a double-bounded distribution, meaning that it is suitable for random processes that are bounded at both their lower and upper ends [79]. The Kumaraswamy formula is fitted to the empirical probability capacity factor values as follows:

$$CF = CF_{min} + \left[1 - (1 - \mathcal{P}^a)^b\right](CF_{max} - CF_{min}) \tag{10}$$

where CF_{min} and CF_{max} are the theoretical lower and upper limits of the capacity factor values, respectively, a and b are shape parameters, and $\mathcal{P}$ is the probability of exceedance. The shape parameters and the limits CF_{min} and CF_{max}, corresponding to $\mathcal{P} \approx 1$ and $\mathcal{P} \approx 0$, are inferred via calibration. We highlight that although the theoretical limits of the capacity factor are 0 and 1, the values of CF_{min} and CF_{max} that are applied in Equation (10), which are inferred through calibration, are much narrower, thus providing a realistic range of capacity factor values for solar energy across Greece. Indeed, the optimized limits of CF under the Kumaraswamy distribution model are 0.17 and 0.23, and they are considered reasonable, according to the authors' experience.

The results of the baseline scenario after fitting the Kumaraswamy distribution are presented in Figure 2. The mean capacity factor of the selected locations (operating in a theoretical centralized setting) is 0.195. Remarkably, accounting for the installed PV capacity over Greece for the year 2022, and the PV power production, i.e., 5788 MW and 8.97 TWh, respectively, the mean capacity factor at the national level equals 0.177, which indicates that the spatial distribution of the selected location quite well reflects the country's PV installations and their performance. The slight overestimation of this analysis' calculated capacity factor is attributed to the fact that a high-efficiency panel is accounted for throughout all simulation lengths. Therefore, the country's old installations that have lower efficiency rates, combined with their respective efficiency reductions due to equipment aging, are not accounted for in the previous comparison.

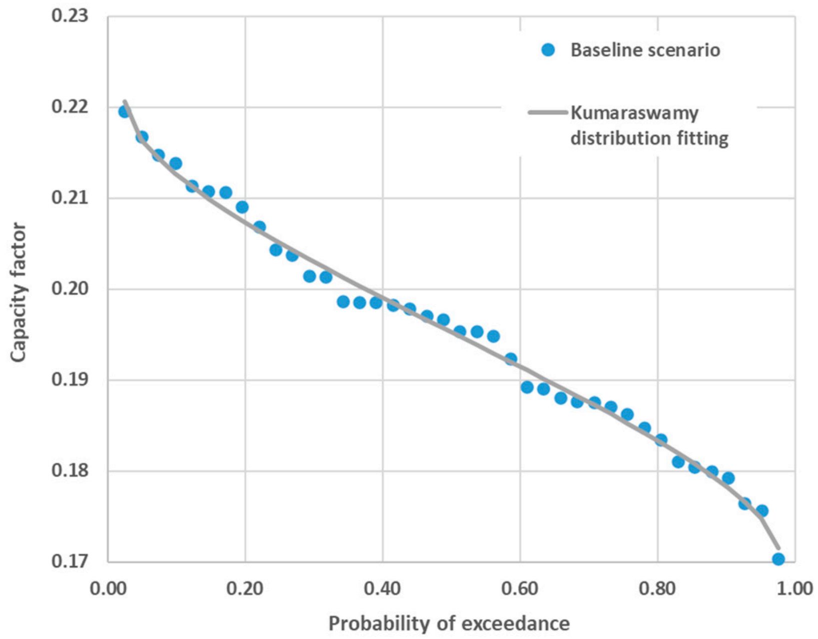

Figure 2. Fitting of the Kumaraswamy distribution function (Equation (10)) to mean annual capacity factors across the 40 points of interest in Greece.

In the context of this research, the exceedance probability is interpreted as a spatial reliability metric. In the baseline scenario, this translates to the number of locations that can guarantee a given level of power production. For instance, a spatial reliability level of 80% dictates that a centralized PV setting of 80% of the selected locations (i.e., 32 out of 40) can guarantee power production that corresponds to a (minimum) capacity factor of approximately 0.185 (as shown in Figure 2). As anticipated, the power output variability between centralized settings is significant, and as such, the sites that exhibit the highest irradiance values are favored.

5.4. Monte Carlo Simulation of Distributed Settings

Section 4 illustrated that the benefits of spatial dispersion of VRES can be demonstrated through the quantification of their spatial reliability. This section depicts this context in practice by assessing PV performance in a distributed (decentralized) setting, employing a Monte Carlo simulation (MCS) approach. The rationale is to calculate the "joint" PV power potential (in terms of the capacity factor) of spatially dispersed sites by distributing the typical panels in equally probable combinations of locations. Each combination is configured by sampling the available number of PV installation sites within the range $[2,\ n-1]$, where n is the total number of feasible locations (40, in the case of this analysis). In order to handle combinatorial explosion and reduce the computational load, 1000 simulations are performed for each setting. Subsequently, exceedance probability curves are produced for all combinations, in which the Kumaraswamy distribution is fitted to the empirically derived data, as shown in Figure 3. Notably, the unit setting refers to the baseline scenario (i.e., fully centralized deployment of solar panels), which has already been investigated in Section 5.2.

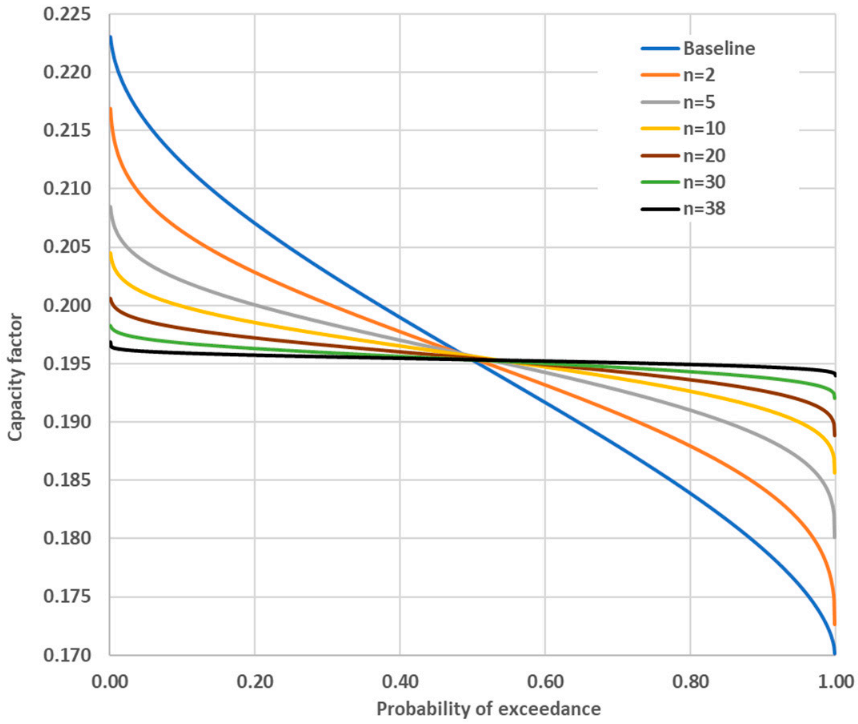

Figure 3. Adjusted theoretical probability curves of the capacity factor for various degrees of PV spatial dispersion (source: created by the authors).

The probabilistic curves provide valuable insights, allowing for a better understanding of PV production capabilities with respect to their spatial dispersion. In the Monte Carlo analysis, spatial reliability refers to the combinations of locations from the total sample that can guarantee a given level of "joint" power production (in terms of capacity factor). It is evident that as more locations are accounted for, and thus, the spatial dispersion of PV configurations increases, the power output variability decreases. As such, this analysis reveals the tradeoff between spatial dispersion and guaranteed power output. Interestingly, the shape of the curves suggests that when the PVs are equally distributed among combinations of the "best" regions and "lesser" performing regions, the guaranteed power output increases. This may be attributed to the spatial decorrelation of meteorological phenomena that induce power curtailment (e.g., cloud coverage, dust accumulation, aerosol concentration, and ozone), provided that the distance between the two locations is substantial. Therefore, centralized settings (and less spatially dispersed ones) exhibit higher production capacities that correspond to lower spatial reliability levels. On the contrary, distributed configurations result in reduced power output variability, thus ensuring higher levels of guaranteed energy yield.

5.5. Derivation of Scale-Reliability-Yield Laws for Solar Energy

In order to provide a better understanding of the tradeoff between PV power output and the issue of scale in the spatial domain, taking advantage of Figure 3 and considering a specific probability of exceedance, the empirically derived capacity factors are plotted, with respect to the number of locations across which PVs are distributed, denoted as a spatial dispersion metric, N. An example is provided in Figure 4a, corresponding to a spatial probability $P = 80\%$. As indicated in the graph, the increase in PV power output follows an asymptotic law, indicating an increasing performance as more locations are accounted for (hence, increasing spatial dispersion). While this increase is quite sharp at the beginning, the following rate of guaranteed power improvement is milder. The same procedure is repeated for five additional values of P, i.e., 85, 90, 95, 97, and 99%, resulting in similar mathematical behavior. In this vein, the asymptotic Gompertz function is fitted to the empirically derived CF values for all spatial probability levels, as follows:

$$CF = CF_{\infty} e^{-bN^{-c}} \tag{11}$$

where CF_{∞} is the theoretical maximum capacity factor value achieved under the fully distributed setting (common for all settings), and b and c are shape parameters that depend on the spatial dispersion metric, N. The aforementioned parameters are inferred via calibration for each reliability level, underlining that all reliability curves should converge to CF_{∞}, when considering a full PV spatial dispersion. This function allows quantification of the scaling law derived from distributed production settings with respect to spatial reliability. The resulting curves illustrated in Figure 4b can be interpreted as the *scale-reliability-yield relationship* for solar energy in Greece.

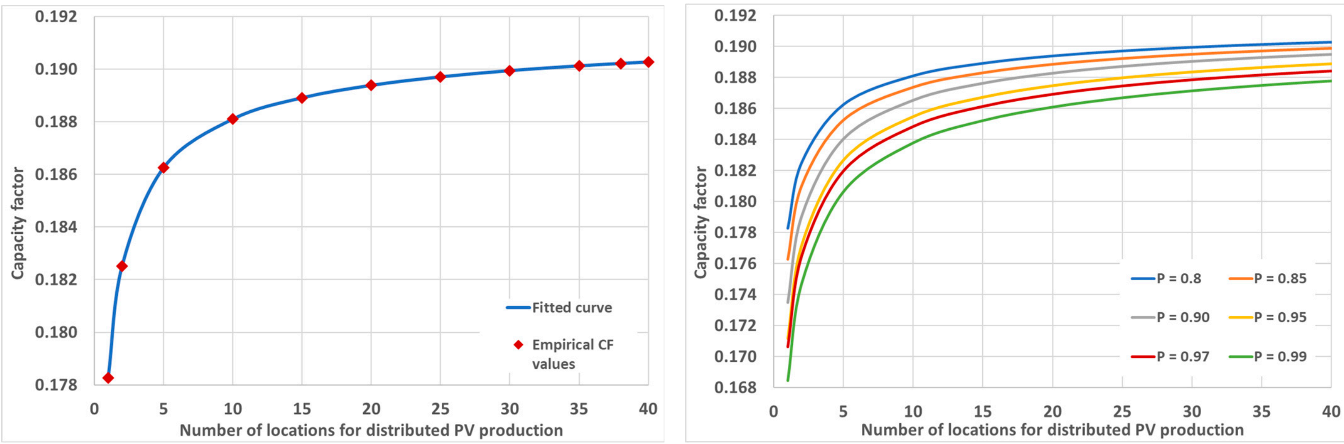

(**a**) (**b**)

Figure 4. (**a**) Fitting of the Gompertz curve to the empirically derived CF values for 80% reliability; (**b**) CF curves for different reliability degrees (source: created by the authors).

Acquiring valuable insights from the graphs, it is evident that the guaranteed PV yield increases when transitioning from centralized to spatially distributed configurations. Conversely, for the same distribution setting, a larger spatial reliability level may be ensured under a decreased guaranteed PV yield. Importantly, the asymptotic CF value is estimated to be up to 0.193, which corresponds to the *optimal guaranteed PV yield in Greece* under a fully distributed setting of solar panels of the examined type. This conclusion is of significant importance for the overall strategic planning of power development at the national level.

6. Discussion

The constantly increasing global population and, consequently, the exponential growth of associated power demand, combined with the goal of rapid decarbonization of the energy sector, have imposed a shift in the traditional paradigms of centralized production systems. Transitioning from conventional configurations, which commonly use fossils, to ones that valorize VRES primarily requires addressing their main bottleneck, namely, their inherited variability and intermittent nature. This is typically addressed by coupling VRES solutions with energy components offering regulation and storage (e.g., hydropower) and by spatially dispersing them under the context of decentralization to decrease power output variability.

In this vein, decentralized systems have been gaining popularity since they can operate either as standalone or grid-connected, providing ancillary services to existing electrical networks. Importantly, both settings of decentralized systems contribute to energy security and enhanced resilience.

This work highlighted the benefits of decentralization under the prism of spatial reliability as a performance metric for the reduction of power output variability. By considering the spatial distribution of solar PVs across Greek territory, it addressed the question, "why shouldn't one simply install all PVs in the "best" performing location?". In reality, the answer lies in the complementarity of spatial and temporal reliability. As such, while the best performing centralized configuration will ensure an overall higher power output, it may not be able to satisfy the load demand at a given time when the underlying weather conditions induce power curtailment (e.g., during an overcast day). On the contrary, spatially dispersed (and thus decorrelated) installations guarantee higher power injections into the grid *at all times* compared to centralized ones. The complementarity between temporal and spatial reliability can be better interpreted through a statistical analysis of hourly power outputs and associated performance metrics (e.g., capacity factors). In this respect, deriving the quantiles of guaranteed power output will allow for assessing reliability as a global concept in two dimensions, i.e., temporal and spatial.

This work utilizes, for the purpose of proof of concept, a typical commercial PV panel to estimate solar power output. As such, it can be reasonably inferred that considering panels with different characteristics (i.e., efficiency and temperature coefficient) would affect the results of this study. Notably, expanding the Monte Carlo framework to also account for the installation of different PV module types across the candidate locations, taking into account aging effects, may result in capacity factor values that better reflect the national one, as per the comparison in Section 5.3.

With regard to strategic PV development over large regions, this work serves as a background feasibility analysis that assesses the overall power output potential of decentralized settings. However, grid integration constraints, such as the inability to absorb all available PV generation due to reduced transmission capacity [80], are not accounted for. Nevertheless, in PV system planning studies, this aspect is essential to consider, as it may dictate both the siting and the sizing of decentralized configurations.

Furthermore, highlighting the complementarity between solar and wind sources, the insights of [39] indicate that a small participation of wind energy (i.e., ~10%) considerably reduces the output generation variability. In this respect, further research should be encouraged to quantitatively assess the spatial reliability of diversified solar PV and wind portfolios.

In a more general economic context, the cost of distributed power systems must account for locational value, as well, when contrasted to that of centralized configurations, since the latter are often deemed as more cost-efficient, exhibiting economies of scale [22]. Locational value is a multi-faceted concept. It can either refer to the energy sector (e.g., lower transmission costs, decreased distribution losses, and enhanced reliability in power delivery) or to general socioeconomic benefits for the associated region (e.g., direct and indirect employment generation stimulated by distributed energy systems). Specifically, for PVs, the additional locational value of distributed systems can be brought by their installation above croplands and arable areas (also termed agrovoltaics), allowing for dual land use and providing additional benefits to both crops (reduced evapotranspiration due to shading effects) and PV modules (reduced cell temperature by creating microclimate conditions below the panels) [81]. In a similar context, the development of floating PVs over distributed open water elements (including hydropower reservoirs) may also be mutually beneficial, resulting in reduced evaporation losses and increased panel efficiency due to cooling [82].

7. Conclusions

This study aimed to investigate the role of spatial scale in the distribution of renewable energy systems. Acknowledging the highly uncertain and stochastic nature of the input parameters used to estimate the power production of VRES systems, their energy yield with respect to spatial dispersion is assessed in probabilistic means by expanding the concept of energy reliability to the space domain, which, to the authors' knowledge, is a subject that has not been previously addressed.

In order to verify this concept, the case of PV development over the Greek territory is considered. A detailed simulation procedure is formulated to assess the PV power output by utilizing the capacity factor metric, while also accounting for the primary factor that significantly affects the overall PV performance (i.e., ambient temperature). A novel Monte Carlo approach is deployed to quantify spatial probabilities, which would otherwise be impossible to estimate analytically. In this vein, PVs are allotted through well-distributed representative combinations of locations, and their "joint" energy yield is estimated. The results of this analysis, expressed in terms of theoretical probabilistic models (in particular, through the Kumaraswamy distribution function), depict a significant reduction in the power output variability that is achieved by spatial dispersion. As such, greater spatial dispersion leads to an increased guaranteed yield for a given spatial reliability. The two bound parameters also have a practical value since they exhibit the range of anticipated capacity factor values across all sites of interest.

The overall outcome is asymptotic-type scale laws to assess the increase in guaranteed energy yield with respect to spatial dispersion. These laws can be interpreted in terms of scale-reliability-yield relationships for solar energy in Greece and reveal the tradeoff between guaranteed PV yield and spatial dispersion. More specifically, the highest guaranteed PV yield for a given spatial reliability is achieved under the fully distributed setting, whereas under the same distribution settings, a larger spatial reliability level may be achieved by decreasing the guaranteed PV yield. A major feature of these scale-reliability-yield curves is their convergence to a common upper value, which denotes the theoretical maximum mean annual capacity factor to be achieved under a fully distributed planning of solar PV energy.

In conclusion, the spatial reliability concept may play a significant role in background feasibility analyses regarding the strategic planning of renewable energy system development, allowing for an initial probabilistic estimation of power output over a given region. As such, decision makers and energy planners can evaluate the necessary degree of PV spatial dispersion for a requested yield under a given reliability level. Importantly, the concept of spatial reliability can also be utilized to assess other sources (e.g., wind and hydropower) or their combined operation (in hybrid systems).

Author Contributions: Conceptualization, A.Z. and A.E.; methodology, A.Z. and A.E.; software, n/a; validation, A.Z and D.C.; formal analysis, A.Z and D.C.; investigation, A.Z and D.C.; resources, n/a; data curation, n/a; writing—original draft preparation, A.Z. and A.E.; writing—review and editing, A.Z. and A.E.; visualization, A.Z and D.C.; supervision, A.E. All authors have read and agreed to the published version of the manuscript.

Funding: This research received no external funding.

Data Availability Statement: The raw weather data (solar radiation and temperature) are publicly available through the PVGIS portal (https://pvgis.com/).

Acknowledgments: A preliminary form of this research was presented at the 2024 European Geosciences Union General Assembly [83].

Conflicts of Interest: The authors declare no conflicts of interest.

Appendix A

Table A1. Coordinates and key annual statistical characteristics of the selected locations.

Location	Latitude (φ)	Longitude (λ)	Mean Solar Radiation (W/m^2)	Mean Temperature (°C)	Mean Annual Capacity Factor
Ioannina	39°35′06″ N	20°55′56″ E	180.33	11.84	0.178
Kastoria	40°28′26″ N	21°12′07″ E	179.81	12.00	0.177
Tripoli	37°29′28″ N	22°24′32″ E	198.15	13.30	0.195
Milos	36°41′30″ N	24°28′31″ E	211.21	18.74	0.211
Kerkira	39°37′57″ N	19°47′47″ E	196.89	17.20	0.195
Crete	35°02′33″ N	24°59′22″ E	219.50	18.28	0.212
Kavala	40°58′05″ N	24°49′12″ E	187.39	15.29	0.186
Larissa	39°33′23″ N	22°31′40″ E	188.88	16.60	0.181
Leivadia	38°26′42″ N	23°01′26″ E	186.92	16.23	0.180
Lesvos	39°07′34″ N	26°19′13″ E	194.72	16.87	0.190
Agrinio	38°36′34″ N	21°20′24″ E	198.42	16.76	0.192
Thessaloniki	40°35′49″ N	22°48′02″ E	186.10	17.08	0.180
Gytheio	36°49′24″ N	22°41′47″ E	210.66	16.36	0.203
Zakynthos	37°45′52″ N	20°50′53″ E	201.22	18.47	0.201
Rhodes	36°21′43″ N	27°58′48″ E	216.68	18.70	0.213
Skyros	38°57′38″ N	24°29′41″ E	195.26	17.48	0.194
Trikala	39°29′36″ N	21°53′08″ E	187.91	15.76	0.180
Evros	40°50′31″ N	25°59′50″ E	187.53	14.74	0.182
Athens	37°58′25″ N	23°47′14″ E	201.33	18.00	0.193
Mykonos	37°25′44″ N	25°19′47″ E	210.53	18.25	0.210
Patra	38°07′40″ N	21°27′16″ E	206.68	17.05	0.200
Serres	40°58′22″ N	23°37′29″ E	184.58	15.97	0.177
Aridaia	40°58′17″ N	22°04′41″ E	180.90	15.37	0.174
Lamia	38°51′44″ N	22°31′16″ E	192.20	17.31	0.183
Chios	38°18′14″ N	26°07′53″ E	208.94	17.91	0.207
Olympia	37°44′35″ N	21°45′27″ E	198.47	15.49	0.192
Kalamata	37°04′02″ N	21°58′35″ E	203.65	18.46	0.196
Corinth	37°55′09″ N	22°53′32″ E	204.27	16.76	0.198
Kozani	40°19′56″ N	21°58′12″ E	183.35	13.26	0.180
Diakopto	38°10′11″ N	22°17′05″ E	198.57	12.95	0.197
Grevena	40°02′44″ N	21°25′25″ E	175.52	13.05	0.172
Karpenisi	38°56′53″ N	21°48′12″ E	176.31	11.61	0.175
Chalkidiki	40°03′51″ N	23°22′09″ E	189.14	17.02	0.187
Drama	41°28′06″ N	24°14′06″ E	170.28	10.62	0.169
Orestiada	41°30′14″ N	26°30′48″ E	179.18	14.71	0.173
Arta	39°05′31″ N	20°59′42″ E	197.75	16.90	0.191
Anafi	36°21′47″ N	25°46′09″ E	214.57	18.92	0.214
Patmos	37°18′36″ N	26°32′53″ E	213.73	18.55	0.213
Limnos	39°54′57″ N	25°10′38″ E	196.53	16.87	0.195
Euvoia	38°33′09″ N	23°45′03″ E	195.24	16.19	0.190

References

1. Jing, J.; Zhou, Y.; Wang, L.; Liu, Y.; Wang, D. The spatial distribution of China's solar energy resources and the optimum tilt angle and power generation potential of PV systems. *Energy Convers. Manag.* **2023**, *283*, 116912. [CrossRef]
2. IRENA. *Renewable Capacity Statistics 2024*; International Renewable Energy Agency: Abu Dhabi, United Arab Emirates, 2024; Available online: https://www.irena.org/Publications/2024/Mar/Renewable-capacity-statistics-2024 (accessed on 11 October 2024).
3. Mouhib, E.; Micheli, L.; Almonacid, F.M.; Fernández, E.F. Overview of the Fundamentals and Applications of Bifacial Photovoltaic Technology: Agrivoltaics and Aquavoltaics. *Energies* **2022**, *15*, 8777. [CrossRef]
4. Li, G.; Li, M.; Taylor, R.; Hao, Y.; Besagni, G.; Markides, C.N. Solar energy utilisation: Current status and roll-out potential. *Appl. Therm. Eng.* **2022**, *209*, 118285. [CrossRef]
5. Tapia, M.; Heinemann, D.; Ballari, D.; Zondervan, E. Spatio-temporal characterization of long-term solar resource using spatial functional data analysis: Understanding the variability and complementarity of global horizontal irradiance in Ecuador. *Renew. Energy* **2022**, *189*, 1176–1193. [CrossRef]

6. Rodríguez-Benítez, F.J.; Arbizu-Barrena, C.; Santos-Alamillos, F.J.; Tovar-Pescador, J.; Pozo-Vázquez, D. Analysis of the intra-day solar resource variability in the Iberian Peninsula. *Sol. Energy* **2018**, *171*, 374–387. [CrossRef]
7. Hofierka, J.; Zlocha, M. A New 3-D Solar Radiation Model for 3-D City Models. *Trans. GIS* **2012**, *16*, 681–690. [CrossRef]
8. Mamassis, N.; Efstratiadis, A.; Apostolidou, I.-G. Topography-adjusted solar radiation indices and their importance in hydrology. *Hydrol. Sci. J.* **2012**, *57*, 756–775. [CrossRef]
9. Hofierka, J.; Kaňuk, J.; Gallay, M. The spatial distribution of photovoltaic power plants in relation to solar resource potential: The case of the Czech Republic and Slovakia. *Morav. Geogr. Rep.* **2014**, *22*, 26–33. [CrossRef]
10. Wang, L.; Lu, Y.; Wang, Z.; Li, H.; Zhang, M. Hourly solar radiation estimation and uncertainty quantification using hybrid models. *Renew. Sustain. Energy Rev.* **2024**, *202*, 114727. [CrossRef]
11. Dubey, S.; Sarvaiya, J.N.; Seshadri, B. Temperature Dependent Photovoltaic (PV) Efficiency and Its Effect on PV Production in the World—A Review. *Energy Procedia* **2013**, *33*, 311–321. [CrossRef]
12. Hassan, Q.; Jaszczur, M.; Przenzak, E.; Abdulateef, J. The PV cell temperature effect on the energy production and module efficiency. *Contemp. Probl. Power Eng. Environ. Prot.* **2016**, *33*, 1.
13. Mekhilef, S.; Saidur, R.; Kamalisarvestani, M. Effect of dust, humidity and air velocity on efficiency of photovoltaic cells. *Renew. Sustain. Energy Rev.* **2012**, *16*, 2920–2925. [CrossRef]
14. Hamdi, R.T.; Hafad, S.A.; Kazem, H.A.; Chaichan, M.T. Humidity impact on photovoltaic cells performance: A review. *Int. J. Recent Eng. Res. Dev.* **2018**, *3*, 27–37.
15. Schnidrig, J.; Chuat, A.; Terrier, C.; Maréchal, F.; Margni, M. Power to the People: On the Role of Districts in Decentralized Energy Systems. *Energies* **2024**, *17*, 1718. [CrossRef]
16. IEA. *Renewables 2019: Analysis and Forecast to 2024*; International Energy Agency: Paris, France, 2019; p. 204. Available online: https://www.iea.org/reports/renewables-2019 (accessed on 16 October 2024).
17. Mills, A.D.; Wiser, R.H. Implications of geographic diversity for short-term variability and predictability of solar power. In Proceedings of the 2011 IEEE Power and Energy Society General Meeting, Detroit, MI, USA, 24–28 July 2011; p. 1.
18. David, M.; Andriamasomanana, F.H.R.; Liandrat, O. Spatial and Temporal Variability of PV Output in an Insular Grid: Case of Reunion Island. *Energy Procedia* **2014**, *57*, 1275–1282. [CrossRef]
19. Riaz, N.; Repo, S.; Lindfors, A.V. Statistical Impact Evaluation of Stochastic Parameters Enhancing Solar Power Inherent Smoothing. In Proceedings of the 2018 IEEE PES Innovative Smart Grid Technologies Conference Europe (ISGT-Europe), Sarajevo, Bosnia and Herzegovina, 21–25 October 2018; p. 1. [CrossRef]
20. Bessa, R.J.; Trindade, A.; Miranda, V. Spatial-Temporal Solar Power Forecasting for Smart Grids. *IEEE Trans. Ind. Inform.* **2015**, *11*, 232–241. [CrossRef]
21. Wang, Q.; Kwan, M.-P.; Fan, J.; Zhou, K.; Wang, Y.-F. A study on the spatial distribution of the renewable energy industries in China and their driving factors. *Renew. Energy* **2019**, *139*, 161–175. [CrossRef]
22. Burger, S.P.; Jenkins, J.D.; Huntington, S.C.; Perez-Arriaga, I.J. Why Distributed?: A Critical Review of the Tradeoffs Between Centralized and Decentralized Resources. *IEEE Power Energy Mag.* **2019**, *17*, 16–24. [CrossRef]
23. Zaihidee, F.M.; Mekhilef, S.; Seyedmahmoudian, M.; Horan, B. Dust as an unalterable deteriorative factor affecting PV panel's efficiency: Why and how. *Renew. Sustain. Energy Rev.* **2016**, *65*, 1267–1278. [CrossRef]
24. Tanesab, J.; Parlevliet, D.; Whale, J.; Urmee, T. Seasonal effect of dust on the degradation of PV modules performance deployed in different climate areas. *Renew. Energy* **2017**, *111*, 105–115. [CrossRef]
25. Psiloglou, B.E.; Kambezidis, H.D.; Kaskaoutis, D.G.; Karagiannis, D.; Polo, J.M. Comparison between MRM simulations, CAMS and PVGIS databases with measured solar radiation components at the Methoni station, Greece. *Renew. Energy* **2020**, *146*, 1372–1391. [CrossRef]
26. Prăvălie, R.; Patriche, C.; Bandoc, G. Spatial assessment of solar energy potential at global scale. A geographical approach. *J. Clean. Prod.* **2019**, *209*, 692–721. [CrossRef]
27. Zhang, Y.; Ren, J.; Pu, Y.; Wang, P. Solar energy potential assessment: A framework to integrate geographic, technological, and economic indices for a potential analysis. *Renew. Energy* **2020**, *149*, 577–586. [CrossRef]
28. Feng, Y.; Zhang, X.; Jia, Y.; Cui, N.; Hao, W.; Li, H.; Gong, D. High-resolution assessment of solar radiation and energy potential in China. *Energy Convers. Manag.* **2021**, *240*, 114265. [CrossRef]
29. Qiu, T.; Wang, L.; Lu, Y.; Zhang, M.; Qin, W.; Wang, S.; Wang, L. Potential assessment of photovoltaic power generation in China. *Renew. Sustain. Energy Rev.* **2022**, *154*, 111900. [CrossRef]
30. Ridha, H.M.; Gomes, C.; Hizam, H.; Ahmadipour, M.; Heidari, A.A.; Chen, H. Multi-objective optimization and multi-criteria decision-making methods for optimal design of standalone photovoltaic system: A comprehensive review. *Renew. Sustain. Energy Rev.* **2021**, *135*, 110202. [CrossRef]
31. Iešmantas, T.; Alzbutas, R. Bayesian spatial reliability model for power transmission network lines. *Electr. Power Syst. Res.* **2019**, *173*, 214–219. [CrossRef]
32. Emara, M.; Filippou, M.C.; Karls, I. Availability and Reliability of Wireless Links in 5G Systems: A Space-Time Approach. In Proceedings of the 2018 IEEE Globecom Workshops (GC Wkshps), Abu Dhabi, United Arab Emirates, 9–13 December 2018; p. 1. [CrossRef]
33. Mendis, H.V.K.; Li, F.Y. Achieving Ultra Reliable Communication in 5G Networks: A Dependability Perspective Availability Analysis in the Space Domain. *IEEE Commun. Lett.* **2017**, *21*, 2057–2060. [CrossRef]

34. Elkadeem, M.R.; Younes, A.; Sharshir, S.W.; Campana, P.E.; Wang, S. Sustainable siting and design optimization of hybrid renewable energy system: A geospatial multi-criteria analysis. *Appl. Energy* **2021**, *295*, 117071. [CrossRef]
35. Carpio, L.G.T. Efficient spatial allocation of solar photovoltaic electric energy generation in different regions of Brazil: A portfolio approach. *Energy Sources Part B Econ. Plan. Policy* **2021**, *16*, 542–557. [CrossRef]
36. Roques, F.; Hiroux, C.; Saguan, M. Optimal wind power deployment in Europe—A portfolio approach. *Energy Policy* **2010**, *38*, 3245–3256. [CrossRef]
37. Tarroja, B.; Mueller, F.; Samuelsen, S. Solar power variability and spatial diversification: Implications from an electric grid load balancing perspective. *Int. J. Energy Res.* **2013**, *37*, 1002–1016. [CrossRef]
38. deLlano-Paz, F.; Calvo-Silvosa, A.; Antelo, S.I.; Soares, I. Energy planning and modern portfolio theory: A review. *Renew. Sustain. Energy Rev.* **2017**, *77*, 636–651. [CrossRef]
39. Mauleón, I. Optimising the spatial allocation of photovoltaic investments: Application to the Spanish case. *Energy Convers. Manag.* **2023**, *291*, 117292. [CrossRef]
40. Markowitz, H. Portfolio Selection. *J. Financ.* **1952**, *7*, 77–91. [CrossRef]
41. Shahriari, M.; Blumsack, S. The capacity value of optimal wind and solar portfolios. *Energy* **2018**, *148*, 992–1005. [CrossRef]
42. Scala, A.; Facchini, A.; Perna, U.; Basosi, R. Portfolio analysis and geographical allocation of renewable sources: A stochastic approach. *Energy Policy* **2019**, *125*, 154–159. [CrossRef]
43. Hu, J.; Harmsen, R.; Crijns-Graus, W.; Worrell, E. Geographical optimization of variable renewable energy capacity in China using modern portfolio theory. *Appl. Energy* **2019**, *253*, 113614. [CrossRef]
44. Bar-Lev, D.; Katz, S. A portfolio approach to fossil fuel procurement in the electric utility industry. *J. Financ.* **1976**, *31*, 933–947. [CrossRef]
45. Schindler, D.; Behr, H.D.; Jung, C. On the spatiotemporal variability and potential of complementarity of wind and solar resources. *Energy Convers. Manag.* **2020**, *218*, 113016. [CrossRef]
46. Weschenfelder, F.; de Novaes Pires Leite, G.; Araújo da Costa, A.C.; de Castro Vilela, O.; Ribeiro, C.M.; Villa Ochoa, A.A.; Araújo, A.M. A review on the complementarity between grid-connected solar and wind power systems. *J. Clean. Prod.* **2020**, *257*, 120617. [CrossRef]
47. deLlano-Paz, F.; Cartelle-Barros, J.J.; Martínez-Fernández, P. Application of modern portfolio theory to the European electricity mix: An assessment of environmentally optimal scenarios. *Environ. Dev. Sustain.* **2024**, *26*, 15001–15029. [CrossRef]
48. Castro, G.M.; Klöckl, C.; Regner, P.; Schmidt, J.; Pereira, A.O. Improvements to Modern Portfolio Theory based models applied to electricity systems. *Energy Econ.* **2022**, *111*, 106047. [CrossRef]
49. Urquhart, B.; Sengupta, M.; Keller, J. Optimizing geographic allotment of photovoltaic capacity in a distributed generation setting. *Prog. Photovolt. Res. Appl.* **2013**, *21*, 1276–1285. [CrossRef]
50. Pillot, B.; Al-Kurdi, N.; Gervet, C.; Linguet, L. An integrated GIS and robust optimization framework for solar PV plant planning scenarios at utility scale. *Appl. Energy* **2020**, *260*, 114257. [CrossRef]
51. Birolini, A. *Reliability Engineering*; Springer: Berlin/Heidelberg, Germany, 2007; Volume 5.
52. Koutsoyiannis, D. Reliability Concepts in Reservoir Design. In *Water Encyclopedia*; John Wiley & Sons, Inc.: Hoboken, NJ, USA, 2005; ISBN 9780471478447.
53. Efstratiadis, A.; Tsoukalas, I.; Koutsoyiannis, D. Generalized storage-reliability-yield framework for hydroelectric reservoirs. *Hydrol. Sci. J.* **2021**, *66*, 580–599. [CrossRef]
54. US Office of Renewable Energy and Energy Efficiency, "Energy Reliability". Available online: https://www.energy.gov/eere/energy-reliability (accessed on 20 October 2024).
55. Singh, S.; Saket, R.K.; Khan, B. A comprehensive review of reliability assessment methodologies for grid-connected photovoltaic systems. *IET Renew. Power Gener.* **2023**, *17*, 1859–1880. [CrossRef]
56. Kahn, E. The reliability of distributed wind generators. *Electr. Power Syst. Res.* **1979**, *2*, 1–14. [CrossRef]
57. Iung, A.M.; Cyrino Oliveira, F.L.; Marcato, A.L.M. A Review on Modeling Variable Renewable Energy: Complementarity and Spatial–Temporal Dependence. *Energies* **2023**, *16*, 1013. [CrossRef]
58. Budischak, C.; Sewell, D.; Thomson, H.; Mach, L.; Veron, D.E.; Kempton, W. Cost-minimized combinations of wind power, solar power and electrochemical storage, powering the grid up to 99.9% of the time. *J. Power Sources* **2013**, *225*, 60–74. [CrossRef]
59. Carden, K.; Wintermantel, N.; Pfeifenberger, J. *The Economics of Resource Adequacy Planning: Why Reserve Margins Are Not Just About Keeping the Lights On*; NRRI Report; National Regulatory Research Institute: Washington, DC, USA, 2011.
60. Tong, D.; Farnham, D.J.; Duan, L.; Zhang, Q.; Lewis, N.S.; Caldeira, K.; Davis, S.J. Geophysical constraints on the reliability of solar and wind power worldwide. *Nat. Commun.* **2021**, *12*, 6146. [CrossRef] [PubMed]
61. de Oliveira, R.; Borges, C.L.T. Influence of photovoltaic generation model and time resolution on the reliability evaluation of distribution systems. *Int. J. Energy Res.* **2021**, *45*, 864–878. [CrossRef]
62. Allan, R.N. *Reliability Evaluation of Power Systems*, 2nd ed.; Plenum Press: New York, NY, USA, 1996.
63. Bromley-Dulfano, I.; Florez, J.; Craig, M.T. Reliability benefits of wide-area renewable energy planning across the Western United States. *Renew. Energy* **2021**, *179*, 1487–1499. [CrossRef]
64. Lian, J.; Zhang, Y.; Ma, C.; Yang, Y.; Chaima, E. A review on recent sizing methodologies of hybrid renewable energy systems. *Energy Convers. Manag.* **2019**, *199*, 112027. [CrossRef]

65. Kumar, S.; Saket, R.K.; Dheer, D.K.; Holm-Nielsen, J.B.; Sanjeevikumar, P. Reliability enhancement of electrical power system including impacts of renewable energy sources: A comprehensive review. *IET Gener. Transm. Distrib.* **2020**, *14*, 1799–1815. [CrossRef]
66. Abunima, H.; Teh, J. Reliability Modeling of PV Systems Based on Time-Varying Failure Rates. *IEEE Access* **2020**, *8*, 14367–14376. [CrossRef]
67. Zisos, A.; Sakki, G.-K.; Efstratiadis, A. Mixing Renewable Energy with Pumped Hydropower Storage: Design Optimization under Uncertainty and Other Challenges. *Sustainability* **2023**, *15*, 13313. [CrossRef]
68. Jurasz, J.; Canales, F.A.; Kies, A.; Guezgouz, M.; Beluco, A. A review on the complementarity of renewable energy sources: Concept, metrics, application and future research directions. *Sol. Energy* **2020**, *195*, 703–724. [CrossRef]
69. Satellite Application Facility on Climate Monitoring (CM SAF). Available online: http://www.cmsaf.eu/EN/Home/home_node.html (accessed on 8 October 2024).
70. Huld, T.; Müller, R.; Gambardella, A. A new solar radiation database for estimating PV performance in Europe and Africa. *Sol. Energy* **2012**, *86*, 1803–1815. [CrossRef]
71. Bakirci, K. Prediction of global solar radiation and comparison with satellite data. *J. Atmos. Sol. -Terr. Phys.* **2017**, *152–153*, 41–49. [CrossRef]
72. Lehneis, R.; Manske, D.; Thrän, D. Generation of Spatiotemporally Resolved Power Production Data of PV Systems in Germany. *ISPRS Int. J. Geo-Inf.* **2020**, *9*, 621. [CrossRef]
73. Jordan, D.C.; Kurtz, S.R. Photovoltaic Degradation Rates—An Analytical Review. *Prog. Photovolt. Res. Appl.* **2013**, *21*, 12–29. [CrossRef]
74. Islam, M.A.; Che, H.S.; Hasanuzzaman, M.; Rahim, N.A. Chapter 5—Energy demand forecasting. In *Energy for Sustainable Development*; Hasanuzzaman, M.D., Rahim, N.A., Eds.; Academic Press: Cambridge, MA, USA, 2020; pp. 105–123. ISBN 978-0-12-814645-3.
75. Correa-Betanzo, C.; Calleja, H.; De León-Aldaco, S. Module temperature models assessment of photovoltaic seasonal energy yield. *Sustain. Energy Technol. Assess.* **2018**, *27*, 9–16. [CrossRef]
76. Evans, D.L.; Florschuetz, L.W. Cost studies on terrestrial photovoltaic power systems with sunlight concentration. *Sol. Energy* **1977**, *19*, 255–262. [CrossRef]
77. Sun, V.; Asanakham, A.; Deethayat, T.; Kiatsiriroat, T. Evaluation of nominal operating cell temperature (NOCT) of glazed photovoltaic thermal module. *Case Stud. Therm. Eng.* **2021**, *28*, 101361. [CrossRef]
78. Sakki, G.K.; Tsoukalas, I.; Kossieris, P.; Makropoulos, C.; Efstratiadis, A. Stochastic simulation-optimization framework for the design and assessment of renewable energy systems under uncertainty. *Renew. Sustain. Energy Rev.* **2022**, *168*, 112886. [CrossRef]
79. Kumaraswamy, P. A generalized probability density function for double-bounded random processes. *J. Hydrol.* **1980**, *46*, 79–88. [CrossRef]
80. Hale, E.T.; Stoll, B.L.; Novacheck, J.E. Integrating solar into Florida's power system: Potential roles for flexibility. *Sol. Energy* **2018**, *170*, 741–751. [CrossRef]
81. Roxani, A.; Zisos, A.; Sakki, G.-K.; Efstratiadis, A. Multidimensional Role of Agrovoltaics in Era of EU Green Deal: Current Status and Analysis of Water–Energy–Food–Land Dependencies. *Land* **2023**, *12*, 1069. [CrossRef]
82. Elminshawy, N.A.S.; Osama, A.; Gagliano, A.; Oterkus, E.; Tina, G.M. A technical and economic evaluation of floating photovoltaic systems in the context of the water-energy nexus. *Energy* **2024**, *303*, 131904. [CrossRef]
83. Chatzopoulos, D.; Zisos, A.; Mamassis, N.; Efstratiadis, A. The benefits of distributed grid production: An insight on the role of spatial scale on solar PV energy. In Proceedings of the EGU General Assembly, Vienna, Austria, 14–19 April 2024. EGU24-3822.